

Uncertainty in assessing the impacts of global change with coupled dynamic species distribution and population models

ERIN CONLISK*, ALEXANDRA D. SYPHARD†, JANET FRANKLIN‡, LORRAINE FLINT§, ALAN FLINT¶ and HELEN REGAN**

*Department of Biology, Center for Conservation Biology, University of California, 900 University Ave, Riverside, CA 92521, USA, †Conservation Biology Institute, 10423 Sierra Vista Ave., La Mesa, CA 91941, USA, ‡School of Geographical Sciences and Urban Planning, Arizona State University, Tempe, AZ 85287-5302, USA, §USGS California Water Science Center, 6000 J Street, Sacramento, CA 95819, USA, ¶USGS California Water Science Center, 6000 J Street, Sacramento, CA 95819, USA, **Department of Biology, University of California, 900 University Ave, Riverside, CA 92521, USA

Abstract

Concern over rapid global changes and the potential for interactions among multiple threats are prompting scientists to combine multiple modelling approaches to understand impacts on biodiversity. A relatively recent development is the combination of species distribution models, land-use change predictions, and dynamic population models to predict the relative and combined impacts of climate change, land-use change, and altered disturbance regimes on species' extinction risk. Each modelling component introduces its own source of uncertainty through different parameters and assumptions, which, when combined, can result in compounded uncertainty that can have major implications for management. Although some uncertainty analyses have been conducted separately on various model components – such as climate predictions, species distribution models, land-use change predictions, and population models – a unified sensitivity analysis comparing various sources of uncertainty in combined modelling approaches is needed to identify the most influential and problematic assumptions. We estimated the sensitivities of long-run population predictions to different ecological assumptions and parameter settings for a rare and endangered annual plant species (*Acanthomintha ilicifolia*, or San Diego thornmint). Uncertainty about habitat suitability predictions, due to the choice of species distribution model, contributed most to variation in predictions about long-run populations.

Keywords: annual plant, climate change, conservation management, coupled model, habitat suitability, invasive plants, land-use change, uncertainty

Received 4 June 2012; revised version received 7 September 2012 and accepted 15 October 2012

Introduction

Species distribution models (SDMs), also called habitat suitability or niche models, are widely used to predict the impact of climate change on species. SDMs predict suitable habitat as a function of environmental variables (Franklin, 2010). However, SDMs do not model populations or their determinants (such as fertility, migration, species interactions, disturbance regimes) beyond habitat suitability. To improve predictions of ecosystem change, coupled models (also called hybrid models) are being developed that integrate SDMs with population models (Keith *et al.*, 2008; Anderson *et al.*, 2009; Lawson *et al.*, 2010; Regan *et al.*, 2011; Conlisk *et al.*, 2012; Dullinger *et al.*, 2012; Fordham *et al.*, 2012a, b). This approach promises better prediction of the

impacts of climate change and related threats to species populations because it considers a wide range of ecological mechanisms simultaneously.

Conservation managers can use these models to assess the impacts of different threats and to rank the importance of different management strategies (Thuiller *et al.*, 2008; Gallien *et al.*, 2010; Midgley *et al.*, 2010). For example, the impact of climate change on habitat suitability can be compared with stressors that act on populations, such as altered fire regimes, spread of exotic competitors, and land-use change. However, coupled models rely on a wide range of data sources and model choices, leading to questions about reliability in the face of compounding uncertainty (Langford *et al.*, 2011). For a coupled model to be an effective management tool, the relative importance of different management options should be robust to model structure and parameterization. As the coupled modelling approach gains traction, exploring model sensitivities to various

Correspondence: Erin Conlisk, tel. + 1 858 776 2939, e-mail: erin.conlisk@gmail.com

model components can provide insights about where the greatest uncertainties lie and about the robustness of decisions informed by the models.

The five main forecasting components in a coupled SDM–population model typically include: (i) climate forecast selection, (ii) choice of SDM, (iii) if and how future land-use change is included, (iv) representation of threats to a population, such as predicted fire return interval, and (v) type of population model and how it is parameterized. Each of these components alone has inherent uncertainty.

Under the A2 ('business as usual') greenhouse gas emissions scenario, the best estimate of globally averaged future temperature increase is 3.4 °C in the next 100 years, but the projected increase among different climate models ranges from 2 to 5.4 °C (IPCC, 2007). This level of temperature uncertainty is small compared with the level of uncertainty in precipitation predictions across the various global climate models (Murphy *et al.*, 2004). Climate predictions serve as input in SDMs used to predict the impact of climate change on the distribution of suitable habitat. Given a specific climate scenario, the choice of SDM can lead to very different suitability predictions. Numerous studies have examined uncertainty in predicted species ranges using different types of SDMs, climate models, and emission scenarios and found that SDM type is the primary source of uncertainty (Thuiller, 2004; Pearson *et al.*, 2006; Buisson *et al.*, 2010). Although ensemble forecasting has been proposed as a solution to this uncertainty (Araújo & New, 2007), other studies showed that carefully evaluating SDMs (e.g., Elith *et al.*, 2010) and comparing only a few models that tend to produce good fits reduces uncertainty greatly (Diniz-Filho *et al.*, 2009).

Different assumptions about regional human population growth and rate of land development lead to uncertainty in forecasting land-use change (Landis & Reilley, 2003). For example, the choice of the historical map used to parameterize urban growth rates and patterns can lead to substantial differences in projected land-use change (Syphard *et al.*, 2011). The speed, type, and location of future land-use change will likely result in substantial changes to fire regimes in Mediterranean ecosystems. As humans both increase ignitions and suppress fires, changes in human population and housing density impact fire frequency and change the spatial distribution of fire (Syphard *et al.*, 2007; Bowman & Murphy, 2010; Medler, 2010). Climate change may also alter fuel moisture, fuel load, and ignition probability (Bowman *et al.*, 2009), potentially altering fire regimes. Previous studies (Keith *et al.*, 2008; Lawson *et al.*, 2010; Regan *et al.*, 2011; Conlisk *et al.*, 2012; Fordham *et al.*, 2012b) exploring the impact of fire frequency on plant

species found that fire frequency had a large effect on population abundance, depending on the species' fire response.

Finally, the type of population model and parameterization can have a strong impact on predicted species abundance. For example, one-stage (or 'scalar') population models tend to predict higher quasiextinction risk than two-stage matrix population models (Dunham *et al.*, 2006). Furthermore, managers often wish to parameterize population models to represent the impact of disturbances, such as fire or the addition of invasive plants, with very limited data. Taylor (1995) and Ludwig (1999) show that estimates of extinction risk are highly uncertain given variability in model input, whereas McCarthy *et al.* (2003) and Brook *et al.* (2000) demonstrate that relative rankings of risks are reliable under parameter uncertainty.

The goal of this study is to determine which of the various model components and parameterizations have the biggest impacts on population predictions. This question is important to land managers and conservation organizations tasked with finding the best management options for protecting biodiversity in the face of global change. Identifying the largest sources of model uncertainty provides guidance in improving a model's value in theoretical and applied contexts. To make this sensitivity analysis relevant to managers, we identify the modelling components with the biggest influence on model predictions through a comparison of the relative impact of climate change, land-use change, altered fire frequency, and invasive species. If changes to the model do not impact the relative importance of these environmental stressors, then we can more confidently use coupled dynamic habitat and population models as a conservation tool.

In particular, we study the endemic annual plant *Acanthomintha ilicifolia*, which is restricted to Southern California, USA, and Baja California, Mexico. This is an ideal case study in which to study compounding uncertainty and the robustness of model outputs. Although the species is well studied in some components (e.g. survival rates), it is poorly understood in others (e.g. responses to fire and extent of suitable habitat for this cryptic annual species). Such uneven knowledge of demography and ecology is typical for species of conservation or management concern. Conservation managers are particularly concerned that frequent fire may negatively affect *A. ilicifolia* by increasing seed bank mortality or promoting invasive plant species (Bauder & Sakrison, 1999). Furthermore, this study uses the coupled model framework to explore a different plant functional type; previous studies focused on obligate seeders and resprouters (Keith *et al.*, 2008; Lawson *et al.*, 2010; Regan *et al.*, 2011; Conlisk *et al.*, 2012; Fordham *et al.*, 2012b).

Materials and methods

SDM predictions of habitat suitability defined the carrying capacities of metapopulation patches, and a demographic model determined the population dynamics within and across the patches. Each model simulation lasted 120 years, where the first 20 years of a run were devoted to 'initial equilibration' before the impact of climate or land-use change began. First, we describe the model components, and then we detail the sensitivity analyses performed.

Current and future suitable habitat maps

We used SDMs to predict the distribution of suitable habitat for *A. ilicifolia* as a function of environmental variables. Species occurrence data were from the California Natural Diversity Database and the Consortium of California Herbaria. The environmental predictors included climate variables (January minimum temperature, mean July maximum temperature, and mean annual precipitation), soil variables, and terrain variables important in determining Southern California plant distributions (Syphard & Franklin, 2009; also see Appendix S1.2 in Supporting Information). Because data for *A. ilicifolia* are sparse (only 104 presence locations were available), we used two machine learning methods, MaxEnt (Phillips *et al.*, 2006) and random forests—hereafter RF (Breiman, 2001; Prasad *et al.*, 2006; Cutler *et al.*, 2007). These widely used methods are robust to small, biased samples (Elith & Graham, 2009), and were chosen to bracket possible differences among SDM predictions. Locations were modelled as 100 m × 100 m grid cells derived from 1971–2000 averaged Parameter-Elevation Regressions on Independent Slopes Model data (PRISM, Daly *et al.*, 2008) and spatially downscaled to a Digital Elevation Model (Flint & Flint, 2012). The bootstrapped accuracy of the habitat suitability models was AUC (area under the curve) = 0.904 for MaxEnt and AUC = 0.870 for RF. Additional details are given in the Supplementary Material (Appendix S1.2).

To project the distribution of future suitable habitat, we substituted future climate variables into the MaxEnt and RF predictor functions estimated from current climate data. We used future climate predictions from two general circulation models—the PCM climate model (from the Department of Energy's Parallel Climate Model) and the GFDL climate model (from the National Oceanic and Atmospheric Association's Geophysical Fluid Dynamic Laboratory's CM.2 model). Predicted climate variables for 2070–2099 were averaged, separately for PCM and GFDL, to represent predicted climate at the end of the century. Averaging over multiple years was done to minimize transient climate differences and because the definition of climate is 30-year average weather. Predicted future climate was statistically downscaled and bias corrected to PRISM data (Flint & Flint, 2012). Finally, to create a time series of suitable habitat maps across 100 years, we linearly interpolated between the current and future maps. We did not consider other emissions scenarios because current trajectories of greenhouse gas emissions are already higher than the most fossil-fuel intensive of the SRES (Special Report on Emission Scenarios) scenarios (Raupach *et al.*, 2007); thus, the only other emissions scenario available with high-resolution climate

projections for our study area (B1) is considered unrealistically low. Also, as SDMs are blind to the source of alternate climate predictions (i.e. different climate models vs. different emission scenarios), considering different emission scenarios would not contribute any further to our understanding of uncertainty in the coupled models. Furthermore, Garcia *et al.* (2012) found that the variability in habitat suitability predictions caused by the emission scenario (B1, A1B, or A2) was roughly equivalent to that of the climate model, with emissions scenarios becoming more important at the end of the century.

To create dynamic projections of urban growth, we used spatially explicit binary projections of urban development from the SLEUTH model, which was carefully calibrated for our study area (Syphard *et al.*, 2011). Urban growth projections were available for the study area for the period 2000–2050. In those projections, the rate of urban growth asymptotes in about 2020, and so predictions beyond 2050 would result in negligible additional growth. This is because the highly urbanized coastal and interior valleys of southern California are surrounded by nondevelopable, mountainous public land. When predicted urban development overlapped otherwise suitable habitat, the areas were declared unsuitable (see Fig. A.1).

Metapopulation patch maps

For a given year, a habitat suitability map assigns a continuous suitability value (ranging from 0 to 1) to each cell. To translate continuous suitability metrics to discrete habitat patches, we selected a threshold value above which we assume that habitat is suitable and below which we assume it is not. The threshold criterion used was the value at which sensitivity (proportion of presences predicted present) plus specificity (proportion of background sample predicted to be unsuitable) is maximized (see Freeman & Moisen, 2008). This threshold criterion was consistent for both MaxEnt and RF. The spatial resolution of the map of known *A. ilicifolia* populations was much finer than that of the model. The 40 hectares of occupied *A. ilicifolia* habitat falls on specific soil types within 481 one-hectare grid cells identified as suitable by our thresholded models. The threshold was 0.37 for the MaxEnt habitat suitability function (at that threshold training Sensitivity = 0.91), and 0.04 for the RF suitability function (Sensitivity = 0.88 and Specificity based on pseudoabsences = 0.75). Threshold values typically differ among SDMs even when the same criterion is used because probability values are scaled differently for different types of models. The results of the SDM model could then be coupled with the population model by transforming the SDM data (gridded landscape made of small cells of varying suitability) into population model data (metapopulation patches), e.g. fields to entities *sensu* Goodchild (1994).

Suitable patches were defined as clusters of five or more adjacent suitable cells. Although populations of *A. ilicifolia* can occur on much smaller soil patches, areas smaller than five cells (or five hectares) were considered too marginal to be suitable habitat for the purposes of these simulations. The carrying capacity of each patch was calculated as the sum of habitat suitabilities over all cells within the patch, multiplied

by a maximum density of 15 000 plants per hectare (Bauder *et al.*, 1994).

As *A. ilicifolia* is not thought to disperse significantly over typical between-patch distances (US Fish and Wildlife Five-Year Review 2009), we did not include between-patch dispersal in the model. However, within-patch dispersal can, in time, have the effect of between-patch dispersal. As climate changes, occupied patches can grow in size, annex previously unsuitable cells, and thus allow *A. ilicifolia* to migrate into previously unsuitable cells. We used the software package RAMAS GIS® 5.0 (Akçakaya and Root 2005) to link the time series of maps to the population model.

Demographic model (two-stage case)

In this case, two life stages are assumed, seeds and adult plants, with both contributing to abundance. In a given year, each plant either dies with no replacement or is replaced by another plant or seed or both, leading to the dynamic:

$$\begin{bmatrix} n_{\text{seed}}(t+1) \\ n_{\text{plant}}(t+1) \end{bmatrix} = C(t) \begin{bmatrix} n_{\text{seed}}(t) \\ n_{\text{plant}}(t) \end{bmatrix} \quad (1)$$

Here $n_{\text{seed}}(t)$ and $n_{\text{plant}}(t)$ are the numbers of seeds and plants in the patch in year t ; and $C(t)$ is a 2×2 matrix of coefficients determining transitions from year t to year $t + 1$. $C(t)$ is assumed to be a random matrix, with each element in each year separately and independently drawn from a lognormal distribution, where the means and standard deviations for the four elements of $C(t)$ are as follows:

$$M = \begin{bmatrix} \mu_{11} & \mu_{12} \\ \mu_{21} & \mu_{22} \end{bmatrix} = \begin{bmatrix} 0.047 & 7.9 \\ 0.11 & 0.80 \end{bmatrix} \quad (2)$$

$$S = \begin{bmatrix} \sigma_{11} & \sigma_{12} \\ \sigma_{21} & \sigma_{22} \end{bmatrix} = \begin{bmatrix} 0.019 & 5.0 \\ 0.072 & 0.70 \end{bmatrix}$$

The randomness of $C(t)$ in Eqn 1 represents environmental stochasticity. The numerical specifications of the mean and standard deviation matrices in Eqn 2 are based on Bauder *et al.* (1994), and Bauder & Sakrison (1997). See Appendix S1 for a detailed description of these parameterizations. To incorporate demographic stochasticity, vital rates for each individual were drawn from a Poisson distribution (for fecundities) or a multinomial distribution (for transition rates) using the patch-specific vital rates matrix.

Demographic model (one-stage case)

The one-stage model is as follows:

$$n_{\text{plant}}(t+1) = c(t)n_{\text{plant}}(t) \quad (3)$$

The coefficient $c(t)$ is assumed to be randomly and independently drawn each year from a lognormal distribution with mean 1.43 and standard deviation 1.05. This mean and standard deviation were chosen for comparability with the corresponding matrices in the two-stage model; the eigenvalues of M and S from Eqn 2 are 1.43 and 1.05. Simulations suggest that comparable abundance growth or decline was achieved using either Eqn 1 or 3. In this part of the study, we are concerned with the effect of population model structure (number

of stages) on model output, rather than the combined effects of model structure and parameter uncertainty. Hence, we use the eigenvalue of the two-stage model to parameterize the one-stage model to ensure comparable parameterization. Below, we consider the effects of parameter uncertainty on population model output, separate from the comparison of model structure. Although a growth factor of 1.43 may appear large, the actual growth rate is constrained by fire (described next) and demographic stochasticity (a high standard deviation in annual growth rates leads to a low geometric mean).

Fire

For each patch and year, the probability of fire was assumed to depend on the time since the last fire according to a discrete time Weibull hazard function:

$$\lambda[T(t)] = cT(t)^{c-1}/b^c \quad (4)$$

Here $\lambda[T(t)]$ denotes the probability of a fire in year t given that the last fire occurred $T(t)$ years earlier; b and c are scale and shape parameters (Polakow *et al.* 1999). We set $c = 1.42$, suggesting a relatively low influence of time since last fire, as is common in chaparral (Polakow *et al.* 1999), which covers the majority of the study area and constitutes the matrix vegetation for *A. ilicifolia*. In simulations, we chose b to represent average fire return intervals from 20 to 80 years, in keeping with historic fire rates (Wells *et al.* 2004). At the start of a simulation, each patch was given an initial value $T(0)$ drawn from the Weibull distribution. Fires were assumed to be spatially independent and to burn entire patches. The largest patch in our model (under the RF-GFDL climate change scenario) was 180,000 hectares, roughly the same size as the six largest (>100,000 ha) southern California fires that have occurred since 2001.

In a year in which a fire occurs, the mean vital rates matrix M (and its eigenvalue 1.43) changes to the following fire matrix F (and its eigenvalue 0.0614):

$$F = \begin{bmatrix} f_{11} & f_{12} \\ f_{21} & f_{22} \end{bmatrix} = \begin{bmatrix} 0.014 & 0.39 \\ 0.011 & 0.0080 \end{bmatrix} \quad (5)$$

The only available information on the impact of fire on *A. ilicifolia* is in qualitative assessments such as those in Bauder & Sakrison (1999): ‘fire during summer or fall could have a detrimental effect on *Acanthomintha* populations by diminishing the seed availability for the next growing season ...’ Thus, the specification of F is highly tentative.

Invasive species

Vegetation managers have noted the spread of the non-native grasses *Brachipodium distachyon*, *Bromus* spp., and *Avena* spp. in *A. ilicifolia* habitat, often following a fire (P. Gordon-Reedy and J. Vinje, personal communication). Thus, we considered two scenarios in which hypothetical competition with other species, described as ‘invasives’, lowers the mean vital rates of *A. ilicifolia* after a fire, thus changing model behavior. In the first scenario, *A. ilicifolia* suffers an immediate postfire disadvantage

relative to invasives. In the first year after a fire, mean fecundity and survival rates of *A. ilicifolia* are assumed to drop to 85% and 90%, respectively, of their baseline values (the elements of M in Eqn 2). The 85% and 90% specifications are based on competition experiments by Bauder & Sakrison (1997). However, as time passes, the vital rates gradually return, over roughly 35 years, to their baseline values. In the second scenario, *A. ilicifolia* has no immediate postfire disadvantage; its mean vital rates start at their baseline values. However, the mean fecundities and survival rates, respectively, gradually decline to 85% and 90% of their baseline values over roughly 25 years as invasives are assumed to encroach and outcompete *A. ilicifolia* (see Appendix S1.8). These two scenarios are based on the speculated impact of fire in Bauder & Sakrison (1997).

Sensitivity analysis

The five model components, and how we varied them in the sensitivity analysis, are as follows:

1. Choice of climate model, specified as either a PCM or a GFDL climate model. The PCM and GFDL models yield contrasting sets of climate predictions for California. PCM predicts a slightly hotter and wetter climate, and GFDL predicts a substantially hotter and drier climate. These models are widely used (Miller *et al.*, 2008; Westerling & Bryant, 2008; Ackerly *et al.*, 2010; Sork *et al.*, 2010) and preferred for climate change impact analysis in California because, while their predictions of historic climate closely match observations, they give contrasting predictions for future climate (Cayan *et al.*, 2008). Thus, the two scenarios bracket the variation that would be found in a large ensemble of climate models.
2. Type of SDM for predicting habitat suitability, either MaxEnt (Elith *et al.*, 2011) or RF (Cutler *et al.*, 2007). We compared MaxEnt and RF because these methods are widely used for predicting climate change impacts (e.g. Iverson *et al.*, 2008; Loarie *et al.*, 2008; Lawler *et al.*, 2009), and perform well in multi-SDM comparisons (Elith *et al.*, 2006; Prasad *et al.*, 2006).
3. Land-use change, either the SLEUTH model of Syphard *et al.* (2011) or no change in current land use.
4. Population model structure, either one stage (plant abundance) or two stages (seed abundance and plant abundance).
5. Population model parameters, either M as in Eqn 2 or $1.25M$ (we doubt that our estimates for the parameters in M would be off by more than 25%).
6. Fire return intervals, one of seven values of the mean fire return interval, plus one no-fire alternative.

Two scenarios are considered for each of 1 to 5, and eight scenarios are considered for component 6, resulting in 256 model variations for exploring uncertainty in forecasts of the effects of future global change. We altered the values in M as opposed to S or F because parameter sensitivity tests showed that the model was most sensitive to values of M . In our additional parameter sensitivity tests we doubled each value in M , S , or F individually for the two-stage population model, PCM climate change, MaxEnt SDM, and land-use change scenario (other scenarios give broadly similar results). We also doubled all values in each matrix simultaneously and compared abundances.

Finally, to place this sensitivity analysis in the context of conservation planning we compared how the relative ranking of four hypothetical management scenarios – land-use change mitigation, fire suppression, competition from invasive plants, and climate change mitigation – depend on different model components (64 models).

Results

Results are presented in terms of ‘average final abundances’ for *A. ilicifolia*—the abundance at the end of each 120-year simulation, averaged over 1000 repetitions of the simulation. When habitat suitability is predicted by RF rather than MaxEnt (Fig. 1), average final abundances are higher across all scenarios (Fig. 2). Average final abundances also increase with fire return interval (Fig. 2). Fewer fires lead to higher abundance for every combination of SDM and population model type. Error bars showing the standard deviation in average final abundance over 11 repetitions of 1000 run sets of simulations are given on Fig. 2a. These error bars are typically smaller than the size of the plotting symbols. This is true for other series on Fig. 2 and on subsequent figures; therefore, we omit further error bars. However, variability from run to run for a given scenario was high, often reflecting the fact that *A. ilicifolia* abundance declines to zero. These results are consistent with observations on *A. ilicifolia*, which show large fluctuations in population size (M. Kelly, unpublished data presented in Appendix S1.5). High reported standard deviations in vital rates data (E. Bauder, personal communication) were used to model environmental stochasticity, where highly variable growth and survival rates lead to extinction across all metapopulation patches in many of the model runs. The coefficient of variation in average final abundance was around three for short FRIs and decreased to roughly 0.25 in the absence of fire. (Appendix Figure S2.2 shows coefficients of variation for the various runs.)

Across all scenarios, average final abundance was higher for the PCM climate model than for ‘no change’ (Fig. 2), resulting from the predicted expansion of suitable habitat (Fig. 1). However, the impact of the GFDL climate model, relative to ‘no change’, depended on which SDM model was used. When the MaxEnt model was used (Fig. 2c,d), the GFDL scenario predicted abundances lower than the ‘no change’ scenario. When the RF model was used (Fig. 2a,b), the GFDL scenario predicted abundances higher than the ‘no change’ scenario. Projected urban growth decreased average final abundance across all scenarios (Fig. 2).

To further illustrate the effects of model components on forecasts of global change, the 256 scenarios were divided into 128 pairs such that each pair corresponded

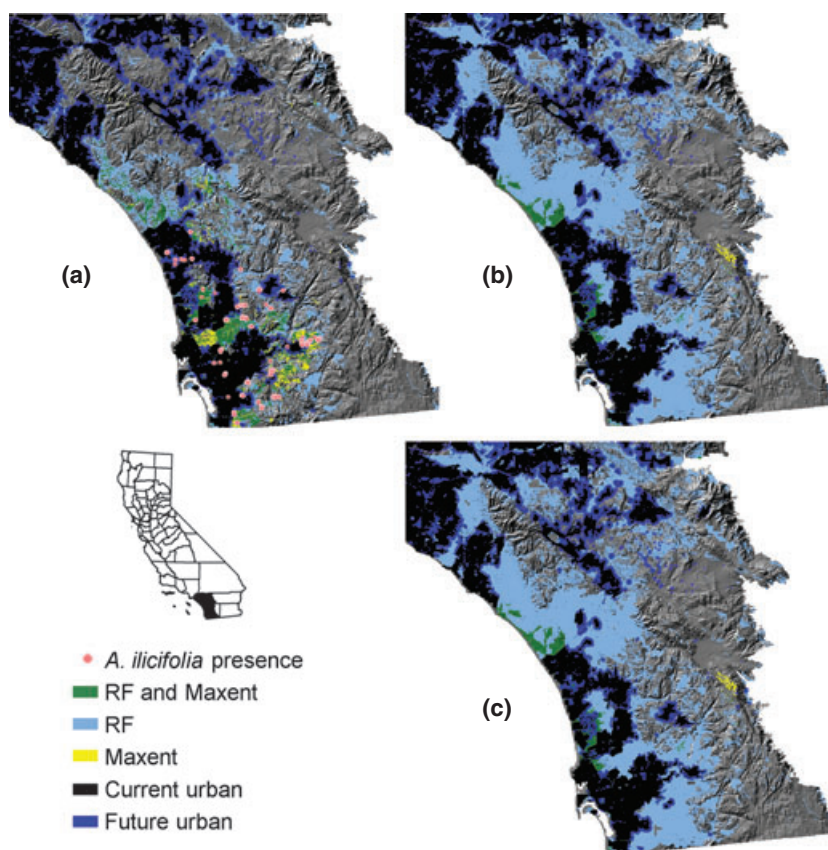


Fig. 1 Map of the study area: most of San Diego and Orange Counties, western Riverside County, and the southern corners of Los Angeles and San Bernardino Counties (see inset). In all three maps, black represents current urban areas, dark blue represents the extent of urban expansion by 2050, yellow represents MaxEnt predicted suitable habitat, light blue represents RF predicted suitable habitat, and green represents suitable habitat predicted by both SDMs. Map (a) shows habitat currently occupied by *Acanthomintha ilicifolia* in pink dots and SDM predictions for the current climate. Map (b) shows predicted 2100 suitable habitat for the PCM future climate scenario. Map (c) shows the same for the GFDL scenario.

to one of five treatments (listed as 1–5 in the Methods): SDM, parameter increase, climate model, land-use change, and population model. Consider SDM choice as an example. For each SDM pair, the average final abundance for the RF treatment was divided by the average final abundance for the MaxEnt treatment, with all other treatments held the same. The resulting 128 ratios are displayed as the column of 128 gray dots on Fig. 3 above the label ‘RF/MaxEnt’. As the average dot height (the black square) and most of the dots individually exceed one, this indicates that RF predicts more favorable habitat scenarios for *A. ilicifolia* than MaxEnt. Likewise, the other columns indicate that increasing M is more favorable to average final abundance than not, that PCM is more favorable than GFDL, that no land-use change is more favorable than land-use change, and that the two-stage population model is slightly more favorable than the one-equation model. Furthermore, the relative heights of the five columns indicate that the average final abundances are most

sensitive to the SDM assumption, second most sensitive to the parameter-level assumption, third most sensitive to the climate change assumption, fourth most sensitive to the land-use assumption, and barely sensitive to population model type.

The following equation summarizes these results as a regression.

$$\begin{aligned} \ln(\text{AveFinalAbundance}) = & 16.92 + 1.59\text{SDM} \\ & (0.091) (0.058) \\ & + 1.20 \text{ParameterIncrease} (0.058) \\ & + 1.18 \text{Climate} - 0.54 \text{LandUseChange} \\ & (0.058) (0.058) \\ & - 0.150 \text{PopModel} + 0.0101 \text{FRI} \\ & (0.058) (0.00097) \end{aligned}$$

Here SDM, ParameterIncrease, Climate, LandUseChange, and PopModel are binary (0 or 1) explanatory variables for the five major contrasts, with 1 corresponding to MaxEnt SDM, a 25% increase in all the vital

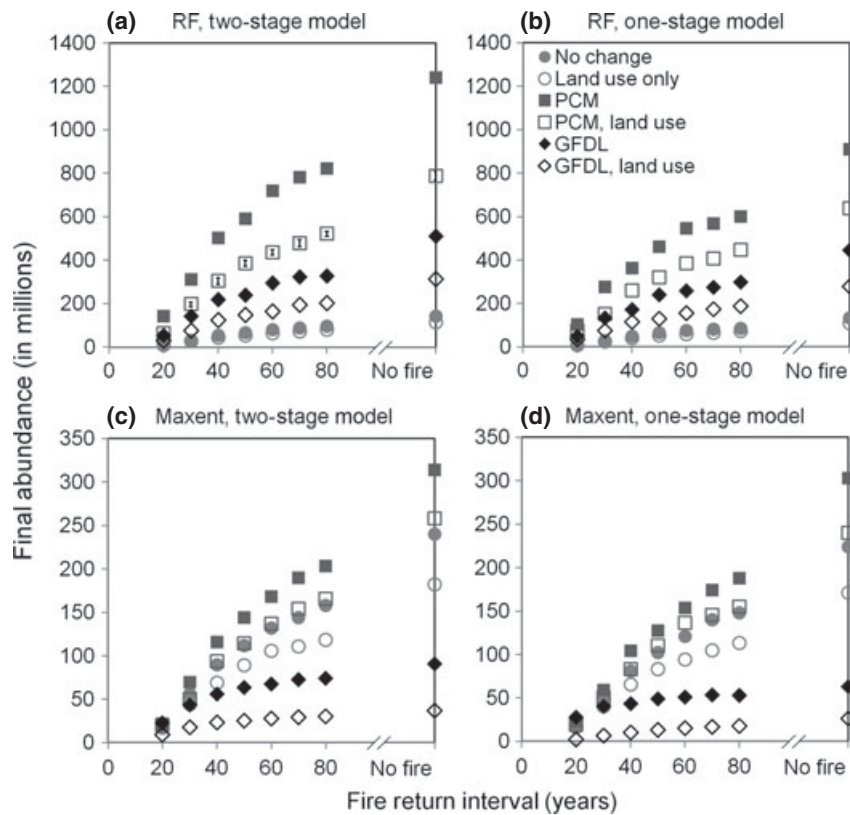


Fig. 2 Average final abundance as a function of average fire return interval for four combinations of SDMs and population models: (a) RF SDM and two-stage population model, (b) RF SDM and one-stage population model, (c) MaxEnt SDM and two-stage population model, and (d) MaxEnt SDM and one-stage population model. Within each panel, the differently labeled points correspond to different climate and land-use change scenarios, as indicated in the legend box superimposed on panel (a). Error bars on the 'PCM, land use' scenario in (a) represent the standard deviation over final abundance. Because the error bars are typically smaller than the size of the plotting symbols (open squares), error bars have been omitted on all subsequent scenarios.

rates in M, PCM climate, land-use change included, and a one-stage population model, respectively. The 'no fire' scenarios of Figs. 2–3 are here replaced by scenarios with FRI = 120 years. With five binary contrasts and eight FRI values (20, 30, 40, 50, 60, 70, 80, 120), the regression sample size is $2^5 \times 8 = 256$ observations. The regression R^2 is 0.88. Estimated standard errors are given in parentheses under the regression coefficients. Because the five binary variables enter the regression in a symmetric way, their standard errors are the same. The variance of the predicted dependent variable on the left equals the weighted sum of the variances of the six uncorrelated explanatory variable terms on the right, where the weights are the squared regression coefficients. Thus, a measure of the importance of an explanatory variable in creating uncertainty about the dependent variable is the explanatory variable's variance times its squared regression coefficient. For the six explanatory variables, these uncertainty measures are 0.64 for SDM, 0.36 for Parameter Increase, 0.35 for Climate, 0.073

for Land-Use Change, 0.0056 for PopModel, and 0.091 for FRI.

Parameter sensitivities are further investigated in Table 1, using the benchmark scenario: two-stage population model, PCM climate model, MaxEnt SDM, and land-use change. Sensitivities are described by changes in 'abundance ratios,' each defined as the ratio of (i) an average final abundance after doubling selected parameters to (ii) the average final abundance for the scenario with no parameter change. Doubling the mean vital rates matrix had the biggest impacts on abundance ratios, followed by the standard deviation matrix and then the fire matrix. The effect of seed survival in the mean vital rates matrix and the effect of fire on vital rates had the smallest impacts, which is fortunate in the sense that these parameters were the least well described by the available data.

Two scenarios in which hypothetical 'invasive species' lower mean vital rates of *A. ilicifolia* after a fire are compared to each other and to scenarios without invasives, assuming MaxEnt or RF SDM, a two-stage model, PCM or GFDL climate change, and land-use change

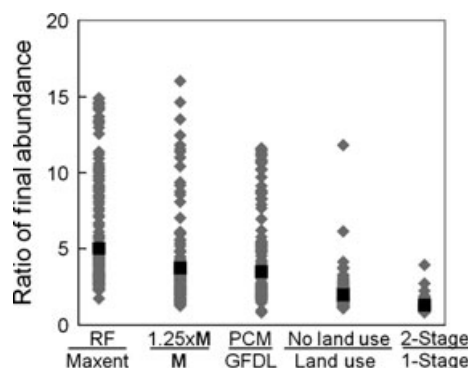


Fig. 3 Sensitivities of final abundances to changes in component scenarios. Each column of dots concerns an all-else-equal change to a component scenario. In the first column, labeled 'RF/MaxEnt', there are 128 specifications for completing the model (by selecting from two climate change options, two land-use change options, two population model options, and eight fire return options) using RF and 128 specifications for MaxEnt. The two lists of 128 abundances for RF and MaxEnt can be paired appropriately (matching specifications) and the ratio of the two average final abundances may be computed (RF in the numerator and MaxEnt in the denominator). The resulting 128 ratios are plotted as the gray diamonds in the first column. The black square, which exceeds one (suggesting that abundances are typically higher for RF simulations), designates the average of the gray dots. The vertical spread of the gray diamonds indicates the distribution of outcomes over the 64 specifications. Parallel interpretations apply to the other four columns.

(Fig. 4). Under both invasive scenarios, competition with the invasives reduces *A. ilicifolia* abundance, with final abundance ratios below one. The first invasive scenario, in which *A. ilicifolia* suffers an immediate postfire disadvantage relative to invasives, has much higher final abundance ratios (Fig. 4a) than the second scenario (Fig. 4b), in which *A. ilicifolia* has no immediate postfire disadvantage but vital rates decline over time since last fire. The ratios of final abundance are highly dependent on FRI in both invasive scenarios. The final abundance ratio of the GFDL–MaxEnt scenario is much higher than for the other scenarios (Fig. 4b). The GFDL–MaxEnt scenario leads to loss of suitable habitat, whereas the other climate–SDM combinations lead to gains in suitable habitat. Thus, abundance decline is primarily driven by declining carrying capacity, not the presence of invasive competitors, and there is a smaller difference between scenarios with and without invasives. Unfortunately, there are no data to determine which invasive scenario is more realistic.

Five hypothetical management options are considered for each of the four climate–SDM combinations coupled with the two-stage population model (Fig. 5). The five management options represent a set of actions leading to climate change mitigation (no further changes in temper-

ature and precipitation), fire suppression, cessation of land-use change (resulting in no further habitat loss due to urban growth), and two kinds of invasive species suppression. The ratio of average final abundance under each management option to average final abundance without that option is shown in Fig. 5. There are large differences in management impacts, indicated by relative bar heights, both across the five options and the four climate–SDM combinations. Rankings of management options are very sensitive to model assumptions. The two PCM scenarios share the same ranking but differ from the GFDL rankings, and the GFDL rankings also differ between SDMs. However, in all climate–SDM combinations, the most important management option is mitigation of invasives when *A. ilicifolia* has the immediate postfire advantage. The management option with the least impact on this species is climate change mitigation. Fire suppression ranks highly in three of four climate–SDM combinations.

Discussion

Although dynamic SDMs coupled with population models make it possible to study the effects of global change on biodiversity, and to compare conservation management strategies, such models involve numerous choices about assumptions and parameters, leading to uncertainties about model results. Sensitivity analyses can shed light on which assumptions and parameter specifications are the most important sources of uncertainties. We present a case study of uncertainty analysis for a model of the endangered species *Acanthomintha ilicifolia* (San Diego thornmint). The main components of our framework are an SDM component, a climate component, a land-use component, a metapopulation model component, and a fire component.

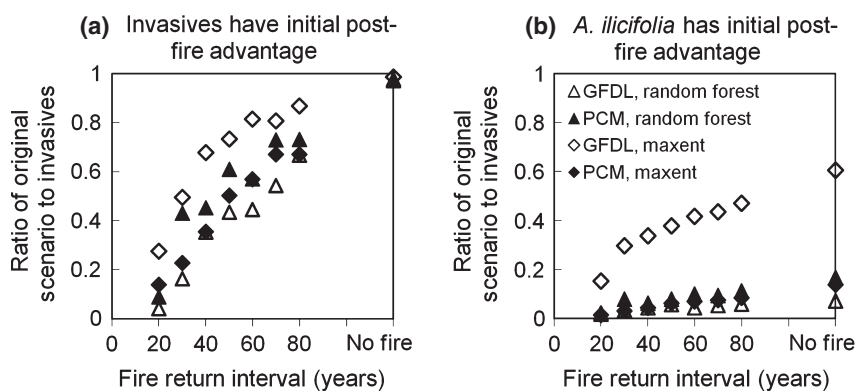
Our results indicate that the SDM component is the most important source of uncertainty, that population model parameter specifications are the next most important, followed by climate change assumptions, fire assumptions, land-use assumptions, and choice of one-stage vs. two-stage population model. Changing the SDM component from MaxEnt to RF has a large effect on predicted *A. ilicifolia* abundance over our 100-year horizon. This result is somewhat surprising as we contrasted only a few carefully constructed models (Elith *et al.*, 2010) and the two machine learning models are among the most accurate SDM techniques (Diniz-Filho *et al.*, 2009). However, substantial variation in results across SDMs used to project species distributions has been well documented (Thuiller, 2004), and in our study the amount and location of suitable habitat had a large impact on population dynamics.

Uncertainty was illustrated in the context of management options for promoting species viability: cessation

Table 1 Population model sensitivities. Sensitivities of abundance ratio to doubling of one or all vital rate : (a) means; (b) standard deviations; (c) for a fire year

	FRI = 20	FRI = 30	FRI = 40	FRI = 50	FRI = 60	FRI = 70	FRI = 80	No Fire
(a)								
μ_{11} : seed survival	1.72	1.69	1.29	1.34	1.27	1.24	1.24	1.13
μ_{12} : seed fecundity	13.72	7.13	4.34	3.78	3.28	3.00	2.83	2.05
μ_{21} : seedling to adult	14.61	7.45	4.40	3.82	3.23	2.95	2.84	2.01
μ_{22} : adult replacement	16.05	7.92	4.72	4.04	3.50	3.17	2.99	2.11
All vital rate means	24.15	10.16	5.63	4.69	3.96	3.52	3.31	2.14
(b)								
σ_{11} : seed survival	0.91	1.01	0.87	0.93	0.94	0.90	0.94	0.94
σ_{12} : seed fecundity	0.13	0.19	0.22	0.27	0.26	0.24	0.29	0.35
σ_{21} : seedling to adult	0.14	0.22	0.23	0.27	0.26	0.28	0.33	0.42
σ_{22} : adult replacement	0.17	0.21	0.23	0.29	0.27	0.30	0.29	0.42
All vital rates std deviations	0	0	0	0.001	0.001	0.001	0.001	0.003
(c)								
f_{11} : seed survival	1.24	1.26	1.10	1.12	1.00	1.05	1.04	1.00
f_{12} : seed fecundity	1.09	1.32	1.04	1.04	1.04	0.98	1.04	1.04
f_{21} : seedling to adult	1.64	1.66	1.28	1.22	1.18	1.12	1.12	1.05
f_{22} : adult replacement	0.91	1.10	0.83	0.99	0.96	0.98	0.99	1.01
All vital rates for fire year	2.20	1.84	1.42	1.29	1.19	1.13	1.09	1.00

Each table entry is a sensitivity of a broad model indicator to an all-else-equal doubling of an underlying vital rate parameter (or set of vital rate parameters), measured at a particular fire return interval, denoted 'FRI'. The broad model indicator is the ratio of (i) the average final abundance for a benchmark climate and land-use change scenario to (ii) the average final abundance for that same scenario, but with a given parameter or set of parameters changed. The benchmark scenario assumes the two-stage population model, MaxEnt SDM, PCM climate model, and presence of land-use change. Thus, the ratios are estimates of how much abundance will change in response to climate and land-use change. A table entry that deviates substantially from one indicates an important parameter to the model.

**Fig. 4** Ratio of (a) average final abundance under a scenario that simulates competition with an invasive species to (b) average final abundance under the same scenario without invasives. The two panels are for two different invasive scenarios described in Methods.

of climate change vs. fire suppression vs. limited land-use change vs. invasive species suppression. Different combinations of SDM, climate, and population model

assumptions led to different effectiveness rankings of these management options. This has implications for using coupled models in decision making. For such

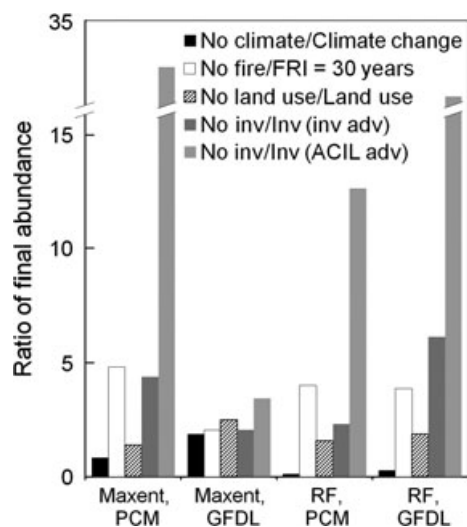


Fig. 5 Ratio of average final abundance under a given 'management option' to average final abundance without the management option, for each of four SDM-climate scenarios (the four sets of five bars each). The management options are climate change mitigation (black bars), fire suppression (white bars), cessation of land-use change (cross-hatch bars), and suppression of invasives (inv) under two assumptions about the behavior of *Acanthomintha ilicifolia* (ACIL) in resisting the invasives (dark and light gray bars). All scenarios assume the two-stage demographic model and, except for the no-fire option, a 30-year average fire return interval. Large differences in relative bar heights indicate that the effects of management options are very sensitive to model assumptions.

models to be useful in conservation, they should be able to reliably predict the stressor with the biggest impact on population viability. Because it is impossible to know, a priori, which SDM is the most appropriate for a given context, the current variability in future suitable habitat predictions makes it difficult to decide between various management options. Although caution must be used when interpreting the results of coupled models, it is important to note that, across all scenarios, reducing the impact of invasives (in the event that *A. ilicifolia* has the postfire advantage) consistently ranked the most beneficial management option. However, the two different invasive scenarios ranked very differently in terms of management efficacy. Thus, the impact of invasives on *A. ilicifolia* is highly uncertain. When the invasive scenarios were not considered, reducing fire frequency consistently ranked among the most beneficial management options across all scenarios.

We do not know which results of this uncertainty analysis for *A. ilicifolia* would carry over to other species. *A. ilicifolia* is a rare, annual plant in a highly urbanized area that may go undetected over much of its range, despite its specialization to distinctive clay soils. The variability in SDM outcomes we report here may

be uncommonly high due to uncertainty in our understanding of the species' current distribution or inability to model its soil specialization. Thus, our study species might be unique. However, we believe that numerous elements of our study would apply to other species. Specifically, we expect that the two SDMs we used would bracket a range of plausible predictions. In a study of habitat suitability predictions under climate change for multiple African taxa, Garcia *et al.* (2012) found that RF predicted the largest habitat gains of any SDM considered. In another study, MaxEnt had greater specificity as compared with RF when used to extrapolate into novel climate conditions (Heikkinen *et al.* 2012). Thus, the optimistic RF model provided a good contrast against the pessimistic MaxEnt model in sensitivity analyses. Regarding climate, we chose two very different climate predictions. The GFDL prediction is considerably hotter and drier than the PCM prediction. These two climate predictions are well established for use in California specifically because they bracket the range of variability that would be found in a larger ensemble of climate predictions (Cayan *et al.*, 2008). Even using such different climate projections, SDMs were a larger source of uncertainty than climate predictions.

It is likely that our results are robust to how we linked SDMs to population models. Our models used SDM suitability predictions to define metapopulation patches and their carrying capacities. Alternatively, we might have used SDM predictions to define other population model parameters, such as vital rates (a novel approach as far as we know). We believe that assigning a strict carrying capacity defined by abiotic resource limitation is the most realistic way to model a wide variety of plant populations, especially *A. ilicifolia*, which is highly dependent on clay soils. Furthermore, SDMs lend themselves straightforwardly to parameterization of carrying capacity, whereas additional assumptions would be required to link SDM predictions to vital rates.

As compared with other annual plants, there is a considerable amount of *A. ilicifolia* life-history data for parameterizing the vital rates matrix M (and less for S and much less for F). These data suggest that growth rates are highly variable between years (see Appendix S1.5). Thus, many of the model runs predicted extinction, whereas other runs predicted that the population was at carrying capacity. For many species that have high growth rates but short lifespans, such variability is common (NCEAS Global Population Dynamics Database). Thus, we do not believe that our results are limited by the life history of *A. ilicifolia*. Regardless, in an effort to exaggerate the impact of changes to life-history parameters as compared with other model components, we dramatically increased the growth and survival

rates of *A. ilicifolia* in our sensitivity analyses. When vital rates were increased, the strict carrying capacity, defined by the SDMs, put a limit on how much the population could grow. Thus, SDMs still led to the most uncertainty in model predictions.

The only model component that rivals SDMs in contributing uncertainty to management options is the impact of invasive species. When invasives are excluded from the analysis, the most effective management option is fire suppression, followed by curbing land-use change for three of the four SDM-climate combinations. The one exception is the MaxEnt-GFDL scenario, for which curbing land-use change is most effective (because much of the suitable habitat predicted by the MaxEnt-GFDL scenario is land slated for urban development). When invasives were included, the two GFDL scenarios differed from one another and from the two PCM scenarios in the ranking of management options. Across all scenarios, the biggest impact on average final abundance is due to invasives in the event that *A. ilicifolia* has the immediate postfire advantage. However, when invasives have the immediate postfire advantage, the relative rank of managing invasives varies for the different SDM-climate scenario combinations. Thus, despite the potential importance of invasives, we cannot define an optimal management option due to the scarcity of data on the impact of invasives.

Similar analyses for other species would be valuable. For reasons detailed above, we might expect SDMs to be the biggest source of uncertainty for other species with better known demographic model parameters and for which the extent of suitable habitat is uncertain due to low detectability and limited dispersal. However, it is possible that variability in SDM predictions for *A. ilicifolia* is due to the species' specialization to clay soils, an association that might make it difficult to separate habitat suitability due to broad-scale environmental predictors from habitat suitability occurring at a finer spatial resolution. Furthermore, we did not explore all of the dozens of available SDMs, climate models, and land-use change scenarios.

Studying more species, SDMs, and climate predictions is an obvious next step. It would also be interesting to consider a range of different model structures across SDMs, climate models, population models, and responses to invasives. The dynamic coupled SDM-population models in this study use regional species distribution data to predict habitat suitability, and thus carrying capacity. Alternatively, population models could be constructed that use local, within-population data to define how growth and survival rates vary as climate changes. If such data became available, the estimated impact of climate change could be based on richer, more detailed local ecological mechanisms. The

impact of climate change as modelled by habitat suitability in coupled models could be compared with the impact of climate change modeled through changing vital rates in a population model.

Acknowledgements

We thank E. Bauder (San Diego State University), J. Snap-Cook (US Fish and Wildlife Service), J. Vinje (Center for Natural Lands Management), P. Gordon-Reedy (Conservation Biology Institute), the San Diego Thornmint Working Group for field observations and background information, and M. Hawke (San Diego Natural History Museum) for distribution data. Special thanks to J. Conlisk and M. Daugherty for discussions about content and presentation. National Science Foundation (NSF-DEB-0 824 708) and Department of Energy (DE-FC02-06ER64159) grants funded this project.

References

- Ackerly DD, Loarie SR, Cornwell WK, Weiss SB, Hamilton H, Branciforte R, Kraft NJB (2010) The geography of climate change: implications for conservation biogeography. *Diversity and Distributions*, **16**, 476–487.
- Akçakaya HR, Root W (2005) *RAMAS GIS: Linking Spatial Data with Population Viability Analysis*. Applied Biomathematics, Setauket, New York.
- Anderson BJ, Akçakaya HR, Araújo MB, Fordham DA, Martinez-Meyer E, Thuiller W, Brook B (2009) Dynamics of range margins for metapopulations under climate change. *Proceedings of the Royal Society B: Biological Sciences*, **276**, 1415–1420.
- Araújo MB, New M (2007) Ensemble forecasting of species distributions. *Trends in Ecology and Evolution*, **22**, 42–47.
- Bauder ET, Sakrison JA (1997) Autecology of San Diego thornmint (*Acanthomintha ilicifolia*). Final report to California Department of Fish and Game, Region 5, Borrego Springs, CA.
- Bauder ET, Sakrison JA (1999) Mechanisms of persistence of San Diego thornmint (*Acanthomintha ilicifolia*). Final Report to California Department of Fish and Game, Region 5, Borrego Springs, CA.
- Bauder ET, McMillan S, Kemp P (1994) *Surveys and assessment of known Acanthomintha ilicifolia populations*. California Department of Fish and Game, Sacramento, CA.
- Bowman DMJS, Murphy B (2010) Australia - a model system for the development of pyrogeography. *Fire Ecology*, **7**, 5–12.
- Bowman DMJS, Blach JK, Artaxo P, Bond WJ, Carlson JM, Cochrane MA (2009) Fire in the Earth System. *Science*, **324**, 481–484.
- Breiman L (2001) Random forests. *Machine Learning*, **45**, 5–32.
- Brook BW, O'Grady JJ, Chapman AP, Burgman MA, Akçakaya HR, Frankham R (2000) Predictive accuracy of population viability analysis in conservation biology. *Nature*, **404**, 385–387.
- Buisson L, Thuiller W, Casajuss N, Lek S, Grenouillet G (2010) Uncertainty in ensemble forecasting of species distribution. *Global Change Biology*, **16**, 1148–1157.
- Cayan DR, Maurer EP, Dettinger MD, Tyree M, Hayhoe K (2008) Climate change scenarios for the California region. *Climatic Change*, **87**, S21–S42.
- Conlisk E, Lawson D, Syphard A, Franklin J, Flint L, Flint A, Regan H (2012) The roles of dispersal, fecundity, and predation on the population of an oak (*Quercus engelmannii*) under global change. *PLoS ONE*, **7**, e36391.
- Cutler DR, Edwards TC Jr, Beard KH, Cutler A, Hess KT, Gibson J, Lawler JJ (2007) Random forests for classification in ecology. *Ecology*, **88**, 2783–2792.
- Daly C, Halbleib M, Smith JI *et al.* (2008) Physiographically sensitive mapping of climatological temperature and precipitation across the conterminous United States. *International Journal of Climatology*, **28**, 2031–2064.
- Diniz-Filho JAF, Bini LM, Rangel TF, Loyola RD, Hof C, Noguez-Bravo D, Araújo MB (2009) Partitioning and mapping uncertainties in ensembles of forecasts of species turnover under climate change. *Ecography*, **32**, 897–906.
- Dullinger S, Gatttringer A, Thuiller W *et al.* (2012) Extinction debt of high-mountain plants under 21st-century climate change. *Nature Climate Change*, **2**, 619–622.
- Dunham AE, Akçakaya R, Bridges TS (2006) Using scalar models for precautionary assessment of threatened species. *Conservation Biology*, **20**, 1499–1506.
- Elith J, Graham C (2009) Do they? How do they? WHY do they differ? On finding reasons for differing performances of species distribution models. *Ecography*, **32**, 1–12.

- Elith J, Graham CH, Anderson RP *et al.* (2006) Novel methods improve predictions of species' distributions with occurrence data. *Ecography*, **29**, 129–151.
- Elith J, Kearney M, Phillips S (2010) The art of modelling range-shifting species. *Methods in Ecology and Evolution*, **1**, 330–342.
- Elith J, Phillips SJ, Hastie T, Dudik M, Chee YE, Yates CJ (2011) A statistical explanation of MaxEnt for ecologists. *Diversity And Distributions*, **17**, 43–57.
- Flint LE, Flint AL (2012) Downscaling future climate scenarios to fine scales for hydrologic and ecological modeling and analysis. *Ecological Processes*, **1**, 1–15.
- Fordham DA, Watts MJ, Delean S, Brook BW, Heard LMB, Bull CM (2012a) Managed relocation as an adaptation strategy for mitigating climate change threats to the persistence of an endangered lizard. *Global Change Biology*, **18**, 2743–2755.
- Fordham DA, Akcakaya HR, Araújo MB, Elith J, Keith DA, Pearson R *et al.* (2012b) Plant extinction risk under climate change: are forecast range shifts an indicator of species vulnerability to global warming? *Global Change Biology*, **18**, 1357–1371.
- Franklin J (2010) *Mapping Species Distributions: Spatial Inference and Prediction*. Cambridge University Press, New York.
- Freeman EA, Moisen CG (2008) A comparison of the performance of threshold criteria for binary classification in terms of predicted prevalence. *Ecological Modelling*, **217**, 48–58.
- Gallien L, Munkemüller T, Albert CH, Boulangeat I, Thuiller W (2010) Predicting potential distributions of invasive species: where to go from here? *Diversity and Distributions*, **16**, 331–342.
- García RA, Burgess ND, Cabeza M, Rahbek C, Araújo MB (2012) Exploring consensus in 21st century projections of climatically suitable areas for African vertebrates. *Global Change Biology*, **18**, 1253–1269.
- Goodchild MF (1994) Integrating GIS and remote sensing for vegetation analysis and modeling: methodological issues. *Journal of Vegetation Science*, **5**, 615–626.
- Heikkinen RK, Marmion M, Luoto M (2012) Does the interpolation accuracy of species distribution models come at the expense of transferability? *Ecography*, **35**, 276–288.
- IPCC (2007) Climate change 2007: The physical science basis. In: *Contribution of Working Group I to the Fourth Assessment Report of the Intergovernmental Panel on Climate Change* (eds Solomon S, Qin D, Manning M, Chen Z, Marquis M, Averyt KB, Tignor M, Miller HL). Cambridge University Press, Cambridge, UK and New York, NY.
- Iverson LR, Prasad AM, Matthews SN, Peters M (2008) Estimating potential habitat for 134 eastern US tree species under six climate scenarios. *Forest Ecology and Management*, **254**, 390–406.
- Keith DA, Akcakaya R, Thuiller W *et al.* (2008) Predicting extinction risks under climate change: coupling stochastic population models with dynamic bioclimatic habitat models. *Biology Letters*, **4**, 560–563.
- Landis JD, Reilly M (2003) How we will grow: Baseline projections of the growth of California's urban footprint through the year 2100. California Energy Commission's working paper 2003-04. Available at: <http://escholarship.org/uc/item/8ff3q0ns;jsessionid=25C33BD3FD724876F0BA0A9B6FDC83A9> (accessed 21 December 2011)
- Langford WT, Gordon A, Bastin L, Bekessy SA, White MD, Newell G (2011) Raising the bar for systematic conservation planning. *Trends in Ecology and Evolution*, **26**, 634–640.
- Lawler JJ, Shafer SL, White D, Kareiva P, Maurer EP, Blaustein AR, Bartlein PJ (2009) Projected climate-induced faunal changes in the Western Hemisphere. *Ecology*, **90**, 588–597.
- Lawson DM, Regan HM, Zedler PH, Franklin J (2010) Cumulative effects of land use, altered fire regime and climate change on persistence of *Ceanothus verrucosus*, a rare, fire-dependent plant species. *Global Change Biology*, **16**, 2518–2529.
- Loarie SR, Carter BE, Hayhoe K, McMahon S, Moe R, Knight CA, Ackerly DD (2008) Climate change and the future of California's endemic flora. *PLoS ONE*, **3**, e2502.
- Ludwig D (1999) Is it meaningful to estimate a probability of extinction? *Ecology*, **80**, 298–310.
- McCarthy MA, Andelman SJ, Possingham HP (2003) Reliability of relative predictions in population viability analysis. *Conservation Biology*, **17**, 982–989.
- Medler MJ (2010) Pyrogeography: Mapping and understanding the spatial patterns of wildfire. *Geospatial Technologies and the Environment*, **3**, 29–47.
- Midgley GF, Davies ID, Albert CH *et al.* (2010) BioMove - an integrated platform simulating the dynamic response of species to environmental change. *Ecography*, **33**, 612–616.
- Miller NL, Hayhoe K, Jin J, Auffhammer M (2008) Climate, extreme heat, and electricity demand in California. *Journal of Applied Meteorology and Climatology*, **47**, 1834–1844.
- Murphy JM, Sexton DMH, Barnett DN *et al.* (2004) Quantification of modelling uncertainties in a large ensemble of climate change simulations. *Nature*, **430**, 768–772.
- NCEAS 2264: Murdoch: Complex Population Dynamics, National Center for Ecological Analysis and Synthesis, and Prendergast J. The Global Population Dynamics Database. [nceas.167.15 \(http://knb.ecoinformatics.org/knb/metacat/nceas.167.15/nceas\)](http://knb.ecoinformatics.org/knb/metacat/nceas.167.15/nceas) (accessed 30 April 2012).
- Pearson RG, Thuiller W, Araújo MB *et al.* (2006) Model-based uncertainty in species' range prediction. *Journal of Biogeography*, **33**, 1704–1711.
- Phillips SJ, Anderson RP, Schapire RE (2006) Maximum entropy modelling of species geographic distributions. *Ecological Modelling*, **190**, 231–259.
- Polakow D, Bond W, Lindenbergh N, Dunne T (1999) Ecosystem engineering as a consequence of natural selection: methods for testing Mutch's hypothesis from a comparative study of fire hazard rates. *Bushfire 99-Australian Bushfire Conference* (eds Lunt I, Green D, Lord B). Charles Sturt University, Albury, Australia.
- Prasad AM, Iverson LR, Liaw A (2006) Newer classification and regression techniques: bagging and random forests for ecological prediction. *Ecosystems*, **9**, 181–199.
- Raupach MR, Marland G, Ciais P, Le Quere C, Canadell JG, Klepper G, Field CB (2007) Global and regional drivers of accelerating CO₂ emissions. *Proceedings of the National Academy of Sciences of the United States of America*, **104**, 10288–10293.
- Regan HM, Syphard A, Franklin J, Swab R, Markovchick L, Flint A *et al.* (2011) Evaluation of assisted colonization strategies under global change for a fire-dependent plant. *Global Change Biology*, **18**, 936–947.
- Sork VL, Davis FW, Westfall R, Flint A, Ikegami M, Wang HF, Grivet D (2010) Gene movement and genetic association with regional climate gradients in California valley oak (*Quercus lobata* Nee) in the face of climate change. *Molecular Ecology*, **19**, 3806–3823.
- Syphard AD, Franklin J (2009) Differences in spatial predictions among species distribution modeling methods vary with species traits and environmental predictors. *Ecography*, **32**, 907–918.
- Syphard AD, Radeloff VC, Keeley JE, Hawbaker TJ, Clayton MK, Stewart SI, Hammer RB (2007) Human influence on California fire regimes. *Ecological Applications*, **17**, 1388–1402.
- Syphard AD, Clarke KC, Franklin J, Regan HM, McGinnis M (2011) Forecasts of habitat loss and fragmentation due to urban growth are sensitive to source of input data. *Journal of Environmental Management*, **92**, 1882–1893.
- Taylor BL (1995) The reliability of using population viability analysis for risk classification of species. *Conservation Biology*, **9**, 551–558.
- Thuiller W (2004) Patterns and uncertainties of species' range shifts under climate change. *Global Change Biology*, **10**, 2020–2027.
- Thuiller W, Albert C, Araújo MB *et al.* (2008) Predicting global change impacts on plant species' distributions: Future challenges. *Perspectives in Plant Ecology Evolution and Systematics*, **9**, 137–152.
- US Fish and Wildlife Five-Year Review, Five-Year Review of *Acanthomintha ilicifolia*: Summary and Evaluation (2009). US Fish and Wildlife Service, Carlsbad Fish and Wildlife Office, Carlsbad, CA.
- Wells ML, O'Leary JF, Franklin J, Michaelsen J, McKinsey DE (2004) Variations in a regional fire regime related to vegetation type in San Diego County, California. *Landscape Ecology*, **19**, 139–152.
- Westerling AL, Bryant BP (2008) Climate change and wildfire in California. *Climatic Change*, **87**, S231–S249.

Supporting Information

Additional Supporting Information may be found in the online version of this article:

Appendix S1. Detailed description of data and methods.
Appendix S2. Additional Figures.